MECHANISM OF THE ^{58,60}Ni(n, p) REACTION AT NEUTRON ENERGIES CLOSE TO 20 MeV

By J. Rondio, A. Korman, B. Mariański and K. Czerski

Sołtan Institute for Nuclear Studies, Warsaw*

(Received September 21, 1988; revised version received February 13, 1989)

The differential cross sections of ^{60}Ni(n, p) reaction were measured at E_n = 17.3 MeV. The results of this and previous investigations of ^{58,60}Ni(n, p) reactions at E_n close to 20 MeV are discussed in terms of the F.K.K. theory and the Geramb model. The determined and calculated total proton emission cross sections are compared.

PACS numbers: 25.40.Eq

1. Introduction

The investigation of neutron induced reactions is difficult because of the low intensities of the available neutron beams and because of the large background. Besides, measurements of the differential cross sections of the (n, p) reaction at neutron energy close to 20 MeV are lacking. The cross sections have been measured for a number of nuclei mainly at neutron energies of about 14–15 MeV, mostly at one or only few angles. So far for many nuclei even the total cross sections have not been determined. Some problems also arise when interpreting the (n, p) reaction mechanism. This mechanism is complicated since different processes have to be taken into account. In this situation new measurements are required at neutron energies close to 20 MeV.

The differential cross sections for the ^{60}Ni(n, p) reaction at incident neutron energy of E_n = 17.3 MeV have been measured and the results are given in the present paper. The experimental angle-integrated proton energy spectrum is shown in Fig. 1. The spectrum can be divided into three energy ranges:

1. The low energy range. Here the emission is described in terms of evaporation from a completely equilibrated nucleus. The compound nucleus wave function which contributes this region is very complex, and involves many different components. Interaction times are long and the statistical considerations are applicable, and lead directly to the evaporation spectrum and an isotropic angular distribution. The spectrum is adequately described by the Weisskopf model [1].

* Address: Instytut Problemów Jądrowych A. Sołtana, Hoża 69, 00-681 Warszawa, Poland.

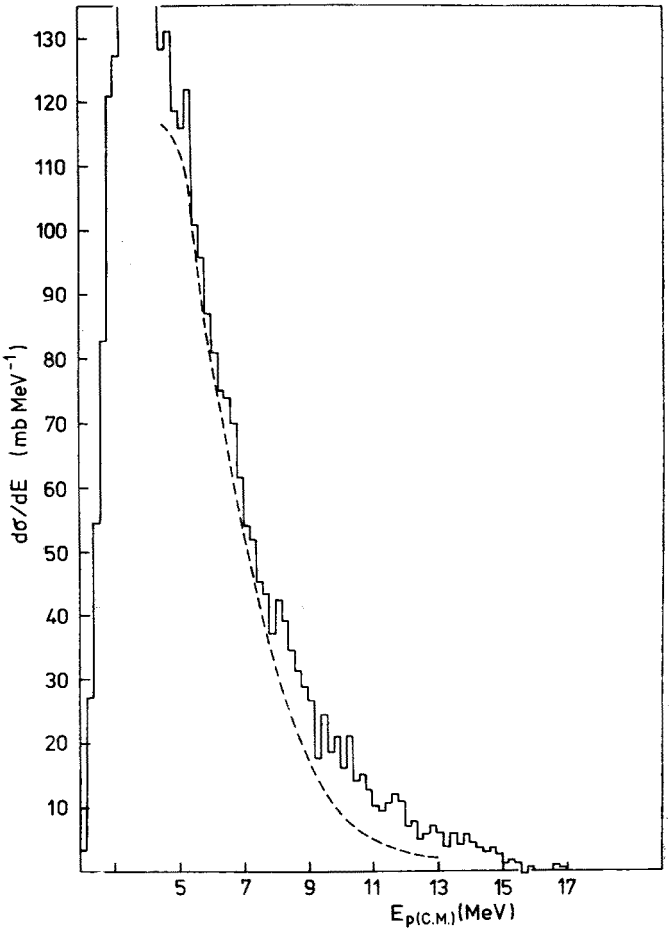

Fig. 1. The experimental angle-integrated proton energy spectrum for the neutron induced reaction on ^{60}Ni at E_n = 17.3 MeV. The broken line represents the compound proton spectrum calculated according to the evaporation formula and normalized to the experimental data

2. The intermediate energy range. The precompound emission is expected to be significant in this range. The exciton model formulated by Griffin [2] and next developed by Blann [3], as well as other models of precompound emission are not yet fully successful.

3. The high energy end of the spectrum. Proton emission is dominated here by the direct transitions to individual states in the final nucleus. They lead to forward peaked angular distributions usually described in the DWBA approximation.

The statistical multistep emission theory formulated by Feshbach, Kerman and Koonin (FKK) [4] assumes that the reaction mechanism is described uniformly for all energies of the emitted particles. The emitting system is considered in terms of the single particle shell model. The excited states are categorized by their number of excitons, which is the sum of the number of particles above the Fermi energy and the number of holes below it. The reaction proceeds through states of increasing exciton number. The spectrum of emitted

particles is calculated by adding the contributions from each stage incoherently. In the F.K.K. theory two kinds of the emission processes are distinquished: The statistical multistep compound (SMCE) ones, and the statistical multistep direct (SMDE) ones.

In the case of SMCE process, in each stage all the particles are bound. In each of the steps of SMDE process, at least one of the particles is in the continuum. In the SMCE process the angle distributions of emission are symmetric about 90°, almost isotropic. When the number of stages is high enough, equilibrium is reached and the statistical emission takes place. On the other hand, the SMDE process in the single step approximation, is equivalent to the direct process.

The statistical emission has been investigated for many years. The precise description of proton spectrum at low energy range is important from our point of view because it allows determination of the total proton emission cross section.

In the intermediate proton energy range we are interested in the interplay between the precompound processes and the excitation of GDR. In the last few years great attention has been paid to the role of giant resonance excitation in nuclear reactions. However, information on this process is rather scarce, especially as regards the neutron induced reactions [5–8]. The precompound contribution was analysed by taking into account both the SMCE and SMDE processes. The possible role of the GDR as a doorway state was tested.

In the high energy range we have investigated the direct transitions to the parent analog states of M1 GDR.

2. Total proton emission cross sections

The precise measurement of the ^{58,60}Ni(n, p) reaction cross sections have been proposed by the IAEA in Vienna in view of the practical aspects of these reactions (nickel is envisaged as a construction material for future fusion reactors). In the (n, p) reaction radiation damages and gaseous hydrogen are produced which presents an important problem.

The experimental equipment and procedure have been described in our previous paper [9]. The experimental set-up used made it possible to measure the two-parameter ΔE-E proton spectra at eight angles simultaneously. Thus the differential cross sections can be obtained for 16 angles in two runs.

The angular integrated proton spectrum measured for the ^{60}Ni(n, p) reaction at 17.3 MeV is shown in Fig. 1. The experimental total proton emission cross section can not be obtained by simple integration of the measured proton spectrum in view of the rapid decrease of the telescope efficiency for proton energies lower than 3–4 MeV. The calculated values were used to estimate the proton emission for these energies. The cross section measured for higher energies was multiplied by the ratio of the cross sections calculated for the suitable energy ranges.

The theoretical cross sections were calculated using the extended EMPIRE code [10] based on the SMCE theory of F.K.K. Gilbert–Cameron level density parameters were used [11] and the spin cut-off parameter was fixed at 1.5. The calculated and measured total proton emission cross sections for the ^{60}Ni(n, p) reaction at E_n = 17.3 MeV are

TABLE I

Total proton emission cross sections

Target nucleus	E_n [MeV]	σ_{exp} [mb]	σ_{theor} [mb]	σ_{np} [mb]	σ_{nnp} [mb]
^{58}Ni	17.3	1172±175	1129	865	264
	18.5	973±145	1122	864	258
^{60}Ni	17.3	527±70	349	217	132
	18.5	403±60	380	228	152

summarized in Table I together with those for ^{58}Ni(n, p) at $E_n = 17.3$ MeV and $E_n = 18.5$ MeV and for Y^{60}Ni(n, p) at $E_n = 18.5$ MeV measured in the previous experiments. The calculated cross sections of the (n, p) (σ_{np}) and (n, np) (σ_{nnp}) reactions are also included in Table I. By the (n, p) reaction we understand all the reactions in which a proton is emitted as the first particle. σ_{np} includes the compound and precompound contributions. σ_{nnp} was computed by assuming that a second particle is emitted from the completely equilibrated nucleus.

The total proton emission cross sections (σ_T) calculated in terms of the F.K.K. SMCE theory do not include the direct contribution so they should be a little lower than the experimental ones. The agreement between the calculated and measured values of σ_T is quite satisfactory. The differences between σ_T measured for the same reaction but at different E_n are close to each other within the limits of experimental error although the values of σ_T measured at $E_n = 17.3$ MeV are greater than those at $E_n = 18.5$ MeV. This is due to the independent normalization used for the different E_n which gives a systematic error in the σ_T determination. This means that the accuracy of our measurements including the systematic errors of normalization is close to the estimated one.

It is difficult to compare the values of σ_T reported here with those obtained in other experiments since the information about the (n, p) reactions at E_n close to 20 MeV is scarce. Some values of σ_{np} and $(\sigma_{nnp}+\sigma_{npn})$ for the ^{58}Ni target nucleus have been determined by the activation method [12–15]. The σ_T values of about 920 mb and 970 mb have been evaluated for this reaction at $E_n = 17.3$ MeV and $E_n = 18.5$ MeV, respectively [16], what is in good agreement with the respective data presented in Table I. The experimental values of σ_T for the ^{60}Ni(n, p) reaction are known only at E_n close to 14 MeV [17]. According to the calculations of Buetner et al. [18] σ_{nnp} is about ten times greater at $E_n = 16$ MeV than at $E_n = 14$ MeV and only a rough estimation of σ_T is possible at $E_n = 17.3$ MeV and $E_n = 18.5$ MeV.

3. Precompound emission of protons

As it was mentioned before, the precompound emission plays a significant role in the intermediate proton energy range. Therefore we separated the spectra of protons emitted due to compound and precompound processes. The calculated compound spectra were

subtracted from the spectra measured for 16 angles. As the calculations including the penetration of the Coulomb barrier by low energy protons are very time consuming, the simple evaporation formulae described in our previous paper [19] were used. In the calculations only the (n, p) and (n, np) reactions were accounted for, the ratio σ_{np}/σ_{nnp} being suitably adjusted. The fitted spectrum is shown in Fig. 1 to illustrate the method. The calculated spectrum is equal to zero for proton energies below the Coulomb barrier and is underestimated close to it. So the calculated spectra were fitted to the measured ones in the 5.5–7.5 MeV energy range. An example of the continuum subtracted proton spectrum in the discussed energy range is shown in Fig. 4. Such spectra were obtained for all 16 angles. The angular distribution of the proton emission in the 8.4–11.8 MeV energy range was obtained on the basis of these spectra.

The angular distribution was discussed in terms of the F.K.K. theory, and the differential SMDE cross sections were calculated for the 8.4–11.8 MeV proton energy range. The calculation was performed according to a single step procedure of the F.K.K. theory given in the form:

$$\frac{d^2\sigma}{dUd\Omega} = \sum_{L} (2L+1)\varrho_2(U)R_2(L)\frac{d\sigma_L}{d\Omega}. \tag{1}$$

The details of the computation are described by Avaldi et al. [20]. The code DWUCK IV of Kunz was used and eight one-particle-one-hole configurations wee accounted for in the calculation. These configurations were formed by the $2p_{3/2}$, $1f_{5/2}$, $2p_{1/2}$, $1g_{9/2}$ and $2d_{5/2}$ one-particle and $1f_{7/2}$, $2s_{1/2}$ and $1d_{3/2}$ one-hole states expected to exist at excitation energies calculated by Ngo Trong et al. [21]. The scheme of these states is shown in Fig. 2. Becchetti–Greenlees optical model parameters [11] were used in the calculation and the spin cut-off parameter σ was fixed at 1.5. The fitted value of the real part of the effective nucleon-nucleon interaction potential $V_0 = 24$ MeV is lower than that usually used, but it is in agreement with those of 25–27 MeV found in the (p, n) reaction [20, 22, 23]. The results of the calculations are presented in Fig. 3. The calculated angular distribution was fitted to the experimental data as the sum of two components: the SMDE component calculated in a single step approximation, as described above, and the isotropic one. The isotropic contribution was noticed during the investigation of the ^{58}Ni(n, p) reaction. It had to be included to obtain a good fit of the experimental angular distribution in the proton energy range corresponding to the transitions to the parent analog states of GDR by the DWBA calculated curve. This contribution has been observed in our investigations of both reactions.

The isotropic contribution may be due to SMCE. A certain form of this process is the proton emission during deexcitation of GDR formed in the doorway state. This process, assumed in our paper [24], was confirmed when the proton spectra at different neutron energies were compared. The energy of the proton emitted in this process is given by the relation:

$$E_P = E_{GDR} - E_b, \tag{2}$$

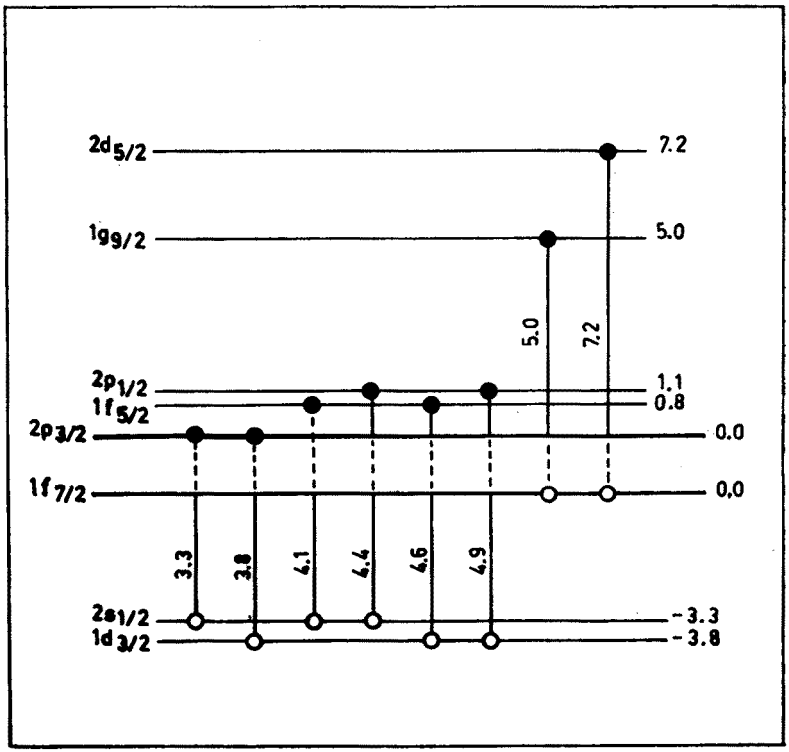

Fig. 2. One-particle-one-hole configurations included to the SMDE calculations for the proton energy range $8.4 < E_p < 11.8$ MeV (3.6–7.0 MeV excitation energy). One-particle neutron states are related to the $2p_{3/2}$ state, one-hole proton states to the $1f_{7/2}$ state

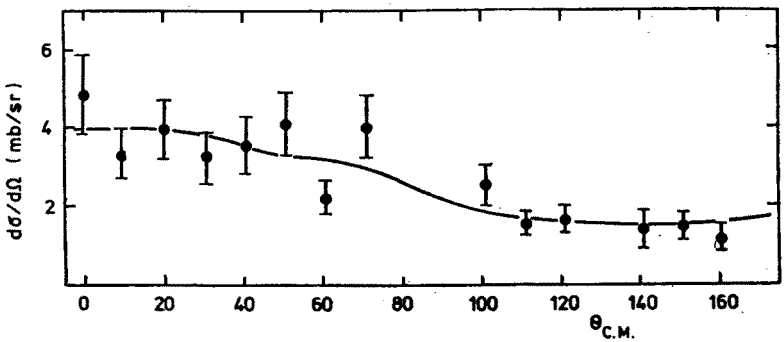

Fig. 3. The measured angular distribution of protons in the energy range of 8.4–11.8 MeV. The solid line represents the results of the single-step calculation of the SMDE process. The isotropic contribution has been also included

where E_b is the binding energy of the proton. From Eq. (2) we see that E_p is independent of the incident neutron energy E_n. The proton energy spectra measured at $E_n = 17.3$ MeV and $E_n = 18.5$ MeV were compared to verify this relation. It has been noticed that for the ^{58}Ni(n, p) reaction the peaks expected to be due to the GDR deexcitation are at the same proton energies for both E_n values [24]. The correlation function for the proton spectra from the ^{60}Ni(n, p) reaction at different E_n was calculated and a maximum was observed for the spectra unshifted in energy [25] which means that E_p of the emitted protons is independent of E_n.

From Eq. (2) it can be expected that the structure of the GDR is imprinted in the proton spectrum. To test this the (n, p) spectrum was compared with the (γ, p) excitation function [26] (see Fig. 4). The correlation function was calculated from the expression

$$R_{xy} = \frac{\sum (x_i y_{i+k}) - \frac{1}{n} \sum (x_i) \sum (y_{i+k})}{\sqrt{\sum (x_i - \bar{x})^2 \sum (y_{i+k} - \bar{y})^2}}, \tag{3}$$

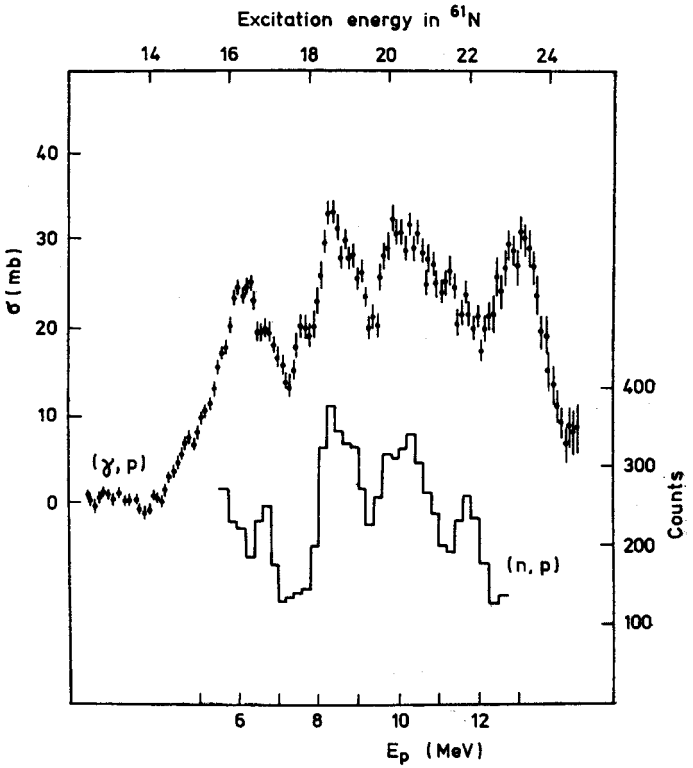

Fig. 4. Comparison of the precompound proton spectrum for the ^{60}Ni(n, p) reaction with the excitation function of the ^{60}Ni(γ, p) photo-reaction. The proton spectrum for the (n, p) reaction is obtained by subtracting the compound nucleus emission from the experimental one and by decreasing statistical fluctuations according to the expression: $\bar{x}_i = \frac{1}{2}[x_i + \frac{1}{2}(x_{i-1} + x_{i+1})]$

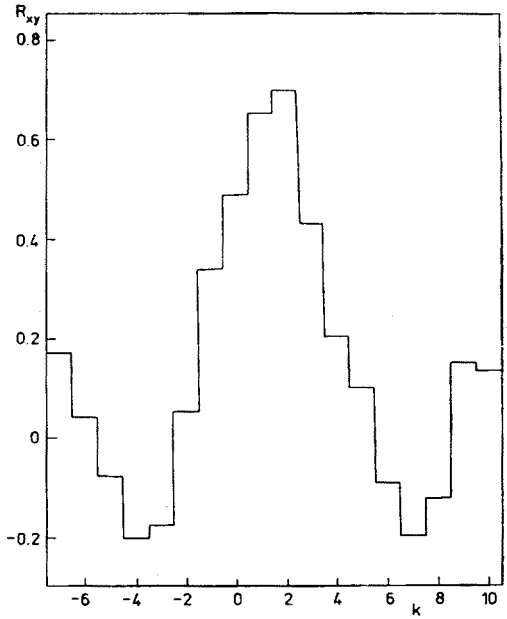

Fig. 5. Correlation function between the spectra presented in Fig. 3. Calculations were performed according to Eq. (3) for $n = 27$ and $k = 0$ for $E_\gamma - E_p = E_b$

where x_i is the number of counts in the i-th channel of the proton spectrum and y_i is $\sigma(\gamma, p)$ in the i-th channel of the excitation function, $\bar{x} = \frac{1}{n}\sum x_i$ and $\bar{y} = \frac{1}{n}\sum y_{i+k}$, is the measured shift of the (γ, p) excitation function energy in relation to the (n, p) spectrum and should be fixed at 0 when $E_\gamma - E_p = E_b$. All sums are over the channels from $i = 1$ to $i = n = 27$, and the correlation function is calculated for the 6.4–11.8 MeV proton energy range. The correlation function presented in Fig. 5 has a great maximum when the shift of the energy scales between E_γ and E_p is by 0.4 MeV greater than the value of E_b. Therefore the results of the experiments confirm the assumption that the isotropic component of the angular distribution is mainly due to the deexcitation of GDR formed in the doorway state by proton emission.

Let us now discuss the next problem. The exhausted fractions of the EWSR for the excitation of the GDR parent analog states were determined in our experiments as the ratio of the experimental β^2,

$$\beta^2 = \frac{\sigma_{GDR}}{2\sigma_{DWBA}} \tag{4}$$

and $\beta^2(100\%)$ calculated from the equation

$$\beta^2(100\%) = \frac{16\pi\hbar^2 NZ}{R^2 2mA^3}\,\frac{1}{E_{exc}}, \tag{5}$$

TABLE II

Sum-rule fractions

Target nucleus	Neutron energy [MeV]	EWSR fraction	
		Without subtraction of the SMDE contribution	With subtraction of the SMDE contribution
^{58}Ni	18.5	135	63
^{58}Ni	17.3	195	115
^{60}Ni	18.5	137	106

TABLE III

Isotropic contributions

Reaction	^{58}Ni(np)		^{60}Ni(np)	
Neutron energy [MeV]	18.5	17.3	18.5	17.3
Proton energy range [MeV]	8.0–14.0	8.0–13.0	6.0–13.0	8.4–13.0
Cross section [mb]	28.9	27.6	30.8	22.6

where σ_{GDR} is determined by fitting the calculated $L = 1$ angular distribution to the experimental data. To get a good fit, an isotropic contribution had to be included and the fit was made as a sum of two components. The obtained fractions of EWSR were significantly greater than 100%, so the SMDE contribution was included as the third component. Now the obtained fractions of EWSR were close to 100% [25].

In our previous papers [19, 24] the EWSR fractions were determined for the ^{58}Ni(n, p) reaction. The angular distributions were fitted as the sum of two components. In this paper new values of the EWSR fractions were determined, the SMDE being included as the third component. The exhausted fractions of EWSR with and without including the SMDE contribution are shown in Table II for both investigated reactions. These results support the assumption that three processes should be taken into account in this proton energy range.

Table III presents the isotropic contributions obtained by fitting the experimental angular distributions by the sum of three components. All the obtained values, as one can see in Table III, are very close to each other.

The processes observed in the ^{58,60}Ni(n, p) reactions are related in a way to the four scattering amplitudes occurring in the Geramb model of inelastic nucleon scattering [27]: The SMDE process corresponds to the direct valence amplitude, the excitation of the GDR parent analog state and the deexcitation of GDR state formed in the doorway state correspond to the resonant amplitude and to the exchange one, respectively [25]. The process corresponding to the direct exchange amplitude is not observed because its effect is small [28].

4. *Parent analog states of M1 GDR*

Two strong excited 1^+ states at 11.87 MeV and 12.34 MeV have been identified in the (e, e') scattering experiments on ^{60}Ni as the M1 GDR states [29]. Analogs of these states can be expected in ^{60}Co at the excitation energies of about 0.74 MeV and 1.21 MeV, respectively

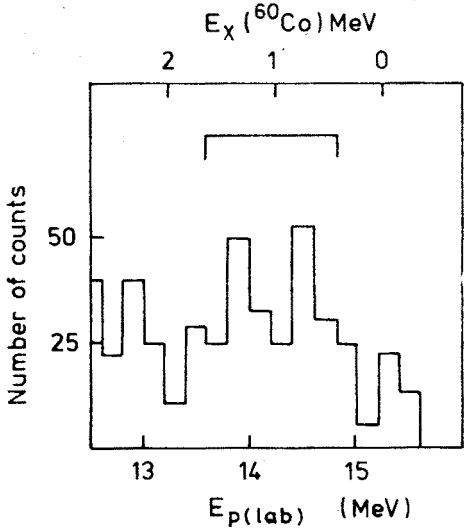

Fig. 6. High energy proton spectrum at 0°

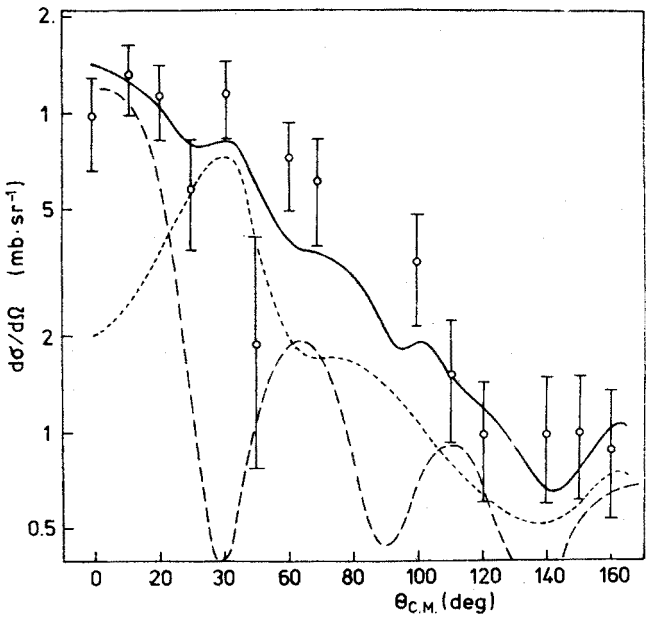

Fig. 7. The measured angular distribution of protons emitted in the 13.6–14.8 MeV energy range. The solid line was obtained as the fitted sum of the DWBA predictions at $L = 0$ (broken curve) and $L = 2$ (dotted curve)

[25]. The two peaks in the proton energy spectrum at about 14.5 MeV and 14.0 MeV, shown in Fig. 6, are expected to be due to the transitions to these analog states. The angular distribution of the proton emission in the 13.6–14.8 MeV energy range is presented in Fig. 7. The experimental angular distribution was fitted as the sum of two DWBA spin-flip transitions with $L = 0$ and $L = 2$.

The observed angular distribution and the proton spectrum are in agreement with those expected for the transitions to the parent analog states of M1 GDR. This is consistent with our previous results for the reactions ^{58}Ni(n, p) and ^{60}Ni(n, p) at $E_n = 18.5$ MeV, which does not mean, however, that the transitions to other states in the final ^{58,60}Co nuclei can be excluded for the discussed proton energy range.

6. *Summary*

The measurements of the differential cross sections of the ^{60}Ni(n, p) reaction at $E_n = 17.3$ MeV are the last in the series of our investigations on the (n, p) reaction mechanism on ^{58,60}Ni isotopes at E_n close to 20 MeV.

The experimental values of σ_T determined for both investigated reactions are compared with the values calculated on the basis of the SMCE theory of F.K.K. The obtained agreement is quite satisfactory.

The interplay of the GDR excitation and the precompound processes was investigated in the intermediate range of proton energies. The obtained experimental results indicate that three processes play a role in the investigated reactions: (*i*) Excitation of parent analog states of E1 GDR, (*ii*) Deexcitation of the GDR formed in the doorway state, and (*iii*) the SMDE. These processes were related to the amplitudes predicted by the Geramb model of inelastic nucleon scattering.

The transitions to parent analog states of M1 GDR were also identified.

REFERENCES

[1] V. F. Weisskopf, *Phys. Today* **14**, 18 (1960).
[2] J. J. Griffin, *Phys. Rev. Lett.* **17**, 478 (1966); *Phys. Lett.* **B24**, 5 (1967).
[3] M. Blann, *Ann. Rev. Nucl. Sci.* **25**, 123 (1975).
[4] H. Feshbach, A. Kerman, S. Koonin, *Ann. Phys.* (USA) **125**, 429 (1980).
[5] J. L. Ullmann, F. P. Brady, C. M. Castaneda, D. H. Fitzgerald, G. A. Needham, J. L. Romero, N. S. P. King, *Nucl. Phys.* **A427**, 493 (1984).
[6] K. Bharuth-Ram, S. M. Perez, F. D. Brooks, S. A. R. Wynchank, W. R. Mc Murray, *Nucl. Phys.* **A278**, 285 (1977).
[7] G. A. Needham, F. P. Brady, D. H. Fitzgerald, J. L. Romero, J. L. Ullmann, J. W. Watson, C. Zanelli, N. S. P. King, G. R. Satchler, *Nucl. Phys.* **A385**, 349 (1982).
[8] W. R. Mc Murray, K. Bharuth-Ram, S. M. Perez, *Z. Phys. A — Atom and Nuclei* **315**, 189 (1984).
[9] B. Mariański, J. Rondio, A. Korman, *Nucl. Instrum. Methods* **206**, 421 (1983).
[10] A. Marcinkowski, Final report to the IAEA on the Research Contract Nr 4326/P. B., Vienna 1987.
[11] A. Gilbert, A. G. W. Cameron, *Can. J. Phys.* **43**, 1146 (1972).
[12] M. Borman, F. Dreyer, U. Zieliński, Rep. EANDC(E) 66 "U" NEA, Paris 1966, p. 42.
[13] P. Decowski, W. Grochulski, A. Marcinkowski, K. Siwek, J. Śledzińska, Z. Wilhelmi, *Nucl. Phys.* **A112**, 513 (1968).

[14] R. Barral, M. Silbergen, D. Gardner, *Nucl. Phys.* **A138**, 387 (1969).
[15] J. M. F. Joronymo, G. S. Mani, J. Olkowsky, A. Sadeghi, C. F. Williamson, *Nucl. Phys.* **47**, 157 (1963).
[16] P. Guenther, A. Smith, D. Smith, J. Whalen, P. Howerton, *Measured and Evaluated Fast Neutron Cross Sections of Elemental Nickel*, ANL/NDM-11, 1975.
[17] A. Chatterjee, *Nucleonics* **23**, 8 (1965).
[18] H. Buetner, A. Lindner, H. Mendner, *Nucl. Phys.* **63**, 625 (1965).
[19] J. Rondio, B. Mariański, A. Korman, *J. Phys. G: Nucl. Phys.* **11**, 549 (1985).
[20] L. Avaldi, R. Bonetti, L. Colli-Millazo, *Phys. Lett.* **94B**, 463 (1980); R. Bonetti, M. Camnasio, L. Colli-Millazo, P. E. Hodgson, *Phys. Rev.* **C24**, 71 (1981).
[21] C. Ngo Trong, T. Suzuki, D. J. Rowe, *Nucl. Phys.* **A313**, 15 (1979).
[22] Y. Holler, A. Kaminsky, R. Langkau, W. Scobel, M. Trabandt, R. Bonetti, *Nucl. Phys.* **A442**, 79 (1985).
[23] E. Mordherst, M. Trabandt, A. Kaminsky, H. Krause, W. Scrobel, R. Bonetti, F. Crespi, *Phys. Rev.* **C34**, 103 (1986).
[24] J. Rondio, B. Mariański, A. Korman, K. Czerski, *Acta Phys. Pol.* **B18**, 1065 (1987).
[25] J. Rondio, B. Mariański, A. Korman, K. Czerski, *Nucl. Phys.* **A487**, 62 (1988).
[26] B. S. Ishkanov, J. M. Kapitonov, J. M. Piskarev, V. G. Schevchenko, O. P. Schevchenko, *Sov. J. Nucl. Phys.* **11**, 272 (1970).
[27] H. V. Geramb, K. Amos, R. Sprinckmann, K. T. Knöpfle, M. Rogger, D. Ingham, C. Mayer-Böricke, *Phys. Rev.* **C12**, 1697 (1975).
[28] W. G. Love, G. R. Satchler, *Nucl. Phys.* **A159**, 1 (1970).
[29] R. A. Lingren, W. L. Bendel, E. C. Jones Jr., L. W. Fagg, X. K. Maruyama, J. W. Linghtbody Jr., S. P. Fivozinsky, *Phys. Rev.* **C14**, 1789 (1974).